RIF1 ensures the organization of replication factories upon DNA replicative stress.

Cyril Ribeyre[1], Marion Larroque[2], Christian Larroque[3] and Angelos Constantinou[1].

[1]Institut de Génétique Humaine (UMR9002), Centre National de la Recherche Scientifique, Université de Montpellier.
141, Rue de la Cardonille, 34396 Montpellier Cedex 5, France

[2]Institut du Cancer de Montpellier, Montpellier, France
208, Avenue des Apothicaires, 34298 Montpellier Cedex 5, France

[3]Institut de Recherche en Cancérologie de Montpellier (U1194), Université de Montpellier, Institut National de la Santé et de la Recherche Médicale
208, avenue des Apothicaires, 34298 Montpellier Cedex 5, France

Correspondence: cyril.ribeyre@igh.cnrs.fr or angelos.constantinou@igh.cnrs.fr

Running title: RIF1 organizes replication factories

Abstract

Eukaryotic genomes are duplicated from thousands of replication origins that fire sequentially forming a defined spatiotemporal pattern of replication clusters. The importance of the organization of replisomes into functional clusters, also called replication factories, is still poorly understood. Here we identified the multifunctional protein RIF1 as a structural component of replication factories. RIF1 depletion did not impair the velocity of replication forks, neither in basic conditions nor in presence of a molecule that interferes with replication fork progression but increased the frequency of DNA lesions induced in S phase. Isolation of replication-associated proteins from RIF1-depleted cells revealed a major defect in the clustering of replication factors on nascent DNA, without any noticeable impact on DNA synthesis or replisome stability. We found that the changes in replication patterns commonly observed upon RIF1 depletion are induced by DNA replication stress. The data suggest that RIF1 encases replication factories to ensure the organization of replication clusters against chromatin rearrangements induced by DNA replication stress.

Keywords: RIF1/replicative stress/nuclear organization/iPOND

Introduction

The duplication of a complete genome is a formidable task that must be perfectly controlled to avoid the transmission to daughter cells of mutations or chromosomal rearrangements. Two meters of DNA are packed and replicated in a human cell of about 10 μm of diameter. Hence, the spatiotemporal program of DNA replication is largely defined by the global organization of the nucleus (Ryba, Hiratani et al., 2010). DNA replication is initiated from defined regions of the genome called origins of replication. More than 30000 replication origins are required for the duplication of the human genome (Mechali, 2010). They are organized in clusters of early and late origins. Within each cluster, stalled forks can be rescued by the firing of nearby dormant origin (Blow, Ge et al., 2011). The timing of replication is impacted by the organization of chromatin loops (Courbet, Gay et al., 2008). Consistent with this, cohesins define the size of chromatin loops and determine replication timing (Guillou, Ibarra et al., 2010). More recently, RIF1, a conserved protein involved in telomeres capping, DNA double-strand break repair and chromatin organization, has been shown to control the timing of DNA replication (Cornacchia, Dileep et al., 2012, Foti, Gnan et al., 2016, Hayano, Kanoh et al., 2012, Mattarocci, Hafner et al., 2016, Yamazaki, Ishii et al., 2012). RIF1 may determine replication timing by at least two means that are linked. First, RIF1 interacts with PP1 phosphatase and could directly impact on origin licensing by counteracting DDK kinases (Dave, Cooley et al., 2014, Hiraga, Alvino et al., 2014, Mattarocci, Shyian et al., 2014). Second, RIF1 interacts with G-quadruplexes and may thereby contribute to the formation of high-order chromatin structures (Kanoh, Matsumoto et al., 2015, Yamazaki, Hayano et al., 2013).

DNA replication is achieved within superstructures called replication factories. They have been described extensively using fluorescence and electron microscopy (Hozak, Hassan et al., 1993, Jackson & Pombo, 1998). Different nuclear patterns of replication factories throughout S phase reflect the orderly and sequential replication of chromatin domains (Dimitrova & Berezney, 2002). To date, the benefit of clustering replication forks into a relative low number of DNA replication factories is not really understood. Replications forks encounter a variety of impediments from both endogenous and exogenous sources (Lambert & Carr, 2013, Zeman & Cimprich, 2014). The slowing or stalling of replication forks induces activation of the checkpoint kinase ATR, which ensures that DNA synthesis within actively replicating chromosomal domains is completed before the duplication of a new chromosomal domain has started. ATR signaling delays the activation of late replication clusters while promoting the firing of dormant origins within active replication clusters (Blow et al., 2011). Hence, the organization of replisomes in clusters is important for the cellular response to replicative stress. Consistent with this, some proteins involved in nuclear organization are also required for the response to replicative stress. For example, Lamin A/C is required for the maintenance of

chromosome integrity when the progression of replication forks is impeded by DNA lesions or nucleotide depletion (Singh, Hunt et al., 2013). Furthermore, the association of Lamin A/C with PCNA is critical for replication forks stability (Cobb, Murray et al., 2016). Hutchinson-Gilford progeria syndrome is caused by a mutation of the LMNA gene that leads to an aberrant Lamin A protein named progerin. The association of progerin with PCNA alters the nuclear distribution of PCNA, induces ATR activation and the formation of γH2A.X (Wheaton, Campuzano et al., 2017). In budding yeast, cohesins accumulate in the vicinity of replication forks upon treatment with hydroxyurea and are required for replication fork restart (Tittel-Elmer, Lengronne et al., 2012). These few examples indicate that links between replicative stress and nuclear structures exist but are still incompletely described.

The isolation of Proteins on Nascent DNA coupled with Mass Spectrometry (iPOND-MS) allows the identification of proteins localized in the vicinity of active replication forks (Aranda, Rutishauser et al., 2014, Dungrawala, Rose et al., 2015, Lopez-Contreras, Ruppen et al., 2013, Lossaint, Larroque et al., 2013, Sirbu, Couch et al., 2011, Sirbu, McDonald et al., 2013). iPOND experiments performed under various experimental conditions have revealed components of the replication machinery (e.g. PCNA and DNA polymerases), proteins that accumulate near forks under stressful conditions (e.g. ATR and FANCD2), and proteins that are required for the restoration of chromatin structures after passage of the replication fork (e.g. histones). Since iPOND involves formaldehyde protein crosslinking, we reasoned that structural components of replication factories may also be captured and identified by iPOND. Consistent with this, Lamin A is detected by iPOND (Wheaton et al., 2017).

Here we identified RIF1 as an important component of replication factories. We show that cells that lack RIF1 exhibit no significant defect in replication fork progression, yet RIF1 is required to limit the accumulation of DNA lesions induced by DNA replication stress. Using iPOND and immunofluorescence microscopy, we demonstrate that RIF1 is required to maintain the organization of replication factories when the progression of replication forks is impaired. We propose that the clustering of replication forks into replication factories limits the formation of DNA lesions caused by DNA replication impediments.

Results

RIF1 localizes near replisomes.

To identify proteins required for the organization of replication factories, we performed iPOND-MS using a highly sensitive last generation mass spectrometer (Sciex TripleTOF 5600+) and quantified the results using MaxQuant (Cox & Mann, 2008). We calculated the LogRatio of the average intensity of peptides isolated immediately after a 5 minutes pulse with EdU divided by the average intensity of peptide isolated after 120 minutes chase with thymidine. As expected, known replisome components such as PCNA, RFC5, Pol Alpha or FEN1 have a LogRatio largely superior to zero indicating that they are indeed associated with ongoing replisomes (Figure 1A). By contrast, histone H4 has a LogRatio close to zero because it does not accumulate near replication forks. We isolated Lamins A/C and Lamins B1 with nascent DNA, both immediately and 120 minutes after EdU labelling of replicated DNA, consistent with a general role for lamins in the organization of nuclear structures. The iPOND-MS data also revealed an enrichment of the cohesins subunits SMC3, SMC1A, STAG2 and PDS5A near forks (Figure 1A), indicating that the iPOND approach also isolates proteins required for the organization of replication factories (Guillou et al., 2010). We noticed that peptides corresponding to RIF1 were also isolated with nascent DNA but not after the chase, suggesting that RIF1 localizes in proximity of active replisomes (Figure 1A), consistent with a recent work performed in *Drosophila melanogaster* (Munden, Rong et al., 2018). Interestingly, it has been proposed that the capacity of RIF1 to associate with G-quadruplexes may underlie its role in the organization of high-order chromatin domains and in the establishment of a replication timing program (Moriyama, Yoshizawa-Sugata et al., 2018). To confirm that RIF1 associates with newly synthesized DNA, we performed iPOND and probed RIF1 by immunoblotting. We detected RIF1 specifically in EdU pulldowns of newly synthesized DNA (Figure 1B). The RIF1 signal was strongly reduced after 120 minutes chase with thymidine, indicating that RIF1 localizes specifically near active replication forks, like PCNA (Figure 1B). We also detected RIF1 in immune-precipitates of endogenous PCNA (Figure 1C). These data indicate that a fraction of RIF1 localizes in the vicinity of active replisomes.

Whereas the depletion of RIF1 in B-lymphocytes and mouse embryonic fibroblasts does not impair the progression of replication forks (Cornacchia et al., 2012, Ray Chaudhuri, Callen et al., 2016), a higher frequency of stalled forks was observed in *rif1*$^{-/-}$ DT40 cells (Xu, Muniandy et al., 2010). To clarify this point, we used a DNA fiber spreading assay in HeLa S3 cells to visualize replication tracts labelled with consecutive pulses of IdU and CldU (SupFig 1A). The length of CldU tracts in RIF1-depleted cells was not considerably different from that of control cells (8.99 μm vs 8.29 μm), indicating that the suppression of RIF1 does not perturb the progression of replication forks. Yet,

several studies have detected the activation of the checkpoint effector kinase Chk1 in RIF1-depleted cells (Chapman, Barral et al., 2013, Foti et al., 2016). We confirmed that Chk1 is phosphorylated on Serine 345 in the absence of RIF1 (Figure 1D). In addition, RPA32 was phosphorylated on Ser4/8, suggesting that RIF1 depleted cells accumulate DNA lesions. The data so far indicate that RIF1 localizes in the vicinity of active replisomes but has no major impact on the progression of replication forks, although the replication checkpoint is constitutively activated in the absence of RIF1.

RIF1 limits the formation of replication-associated DNA lesions.

In an attempt to reveal the function of RIF1 at replication forks, we used the DNA polymerase inhibitor aphidicolin (APH) to induce DNA replication stress. We pulse labelled HeLa S3 cells for 30 minutes with IdU and then for 30 minutes with CldU in presence of a low dose (0.05 μM) of APH. As expected, the ratio of the lengths of CldU versus IdU tracts was close to 1 in control conditions and reduced by half in presence of APH (Figure 2A). The status of RIF1 did not change the ratios of CldU/IdU tracts (Figure 2A). This result indicates that RIF1 does not influence the progression of replication forks in presence or replicative stress. The presence of RIF1 in the vicinity of replication forks could be related to its ability to protect hydroxyurea-stalled forks from DNA resection by nucleases (Garzón, Ursich et al., 2019, Ray Chaudhuri et al., 2016). To test if we can reproduce this observation with APH we treated cells 6 hours with a high dose (1 μM) of APH after 30 min labelling of IdU and CldU and measured the ratio between CldU and IdU. As expected the ratio was close to 1 in cells treated with a control siRNA, and bellow 1 in RIF1 depleted cells(Figure 2B). This confirms that RIF1 is protecting stalled forks from resection. To test if the loss of DNA protection upon RIF1 supression is leading to the formation of DNA lesions, we analyzed the percentage of γ-H2A.X positive cells upon 24 hours of treatment with APH. We found that the frequency of γ-H2A.X-positive cells is almost 2 fold higher (47% vs 25%) in absence of RIF1 compared to control (Figure 2C). These results are consistent with the higher sensitivity of *rif1*$^{-/-}$DT40 cells to aphidicolin and hydroxyurea (Buonomo, Wu et al., 2009, Xu et al., 2010). Altoghether, our data suggest that RIF1 is present at replication forks to limit the accumulation of DNA lesions in response to replicative stress.

RIF1 depletion reduces iPOND pull down efficiency without affecting EdU incorporation and replisome stability.

Since the suppression of RIF1 does not impair DNA synthesis at the level of individual replication forks (Figure 2A and SupFig 1A), we surmised that RIF1 could play a role in the organization of replication factories that is important to limit the accumulation of replication-associated DNA lesions. This is based on several observations demonstrating that RIF1 is involved in nuclear organization (Foti et al., 2016, Moriyama et al., 2018, Yamazaki et al., 2012). Interestingly, in the Foti et al. study the

authors used conformation capture sequencing (4C-seq) to show the impact of RIF1 impairment on nuclear architecture. Chromosome conformation capture techniques use formaldehyde-crosslinking to freeze and quantify proximal DNA regions (Dekker, Rippe et al., 2002) and replication factories appear as EdU-labelled nuclear foci by immunofluorescence staining. We reasoned that since iPOND uses formaldehyde-crosslinking, the pulldown of EdU-labeled DNA should capture clusters of replication forks assembled into replication factories. It follows that the iPOND method should not only isolate components of the replication machinery but also structural components of replication factories. Furthermore, the efficacy of protein isolation by iPOND should correlate directly with the density of replication clusters that are "frozen" by formaldehyde crosslinking (Figure 3A).

To explore the function of RIF1 in the organization of replication clusters, we performed iPOND using stable control and RIF1-depleted HeLa S3 cells (Figure 3B). In basal conditions, the efficiency of PCNA isolation with nascent DNA was similar in control and RIF1-depleted cells. As expected, cellular treatment with a low dose of APH (0.1 μM) induced the recruitment of BRCA1 and TopBP1 on nascent DNA (Figure 3C). Strikingly, the yield of PCNA, BRCA1 and TopBP1 isolated from RIF1-depleted cells treated with APH diminished dramatically and reproducibly. To establish further this observation, we isolated EdU-bound proteins after recovery from an APH treatment (Figure 3D). We treated cells with 0.1 μM APH for 30 minutes and then washed the cells free of the drugs and labelled nascent DNA for 30 minutes with EdU. In comparison with control cells (shLUC), the isolation of RIF1, PCNA, MCM7 and MSH2 with nascent DNA from RIF1-depleted cells was dramatically reduced (Figure 3D). DNA fibers labelling experiments, however, revealed that replication forks in RIF1-depleted cells progress at the same rate as in control cells, and are similarly slowed-down by APH treatment (Figure 2A, B and SupFig2A). Thus, a defect in DNA synthesis does not account for the reduced isolation of EdU-bound proteins from RIF1-depleted cells. Consistent with this, RIF1 suppression had no impact on the level of EdU incorporation per nucleus, under basal conditions and upon APH treatment (SupFig2B). Furthermore, we detected similar levels of the replisome-associated proteins MSH2 and MCM7 in PCNA immune-precipitates from control and RIF1-depleted cells (SupFig 3C), suggesting that RIF1 is not required for replisome stability. Collectively, these data indicate that RIF1 is not necessary for replisome stability and replication fork progression. The reduced yield of protein capture by iPOND in RIF1-depleted cells rather suggests that RIF1 has an impact on replication forks clustering. To consolidate this observation, we coupled iPOND to mass spectrometry and used MaxQuant for label-free quantification analyses. Importantly, we did not normalize samples in order to detect variations in protein abundance. Quantification of mass spectrometry data confirmed western blot analyses of PCNA pulldowns from control and RIF1 depleted cells (Figure 3E). As for PCNA, the treatment of RIF1-depleted cell with APH markedly reduced the abundance of the replication factors MSH6, DPOD1, FEN1 and RFC4 captured by iPOND (Figure 3E).

By contrast, changes in the efficiency of streptavidin pulldowns were not observed for mitochondrial proteins such as NDUS1, NDUS3, P5CR2 and SDHA, which are also isolated by iPOND (Figure 3F). To generalize this observation to the whole replisome, we summed the peptides intensities of all replisome proteins listed in a previous study (Lopez-Contreras et al., 2013)(Figure 3G). In control cells (shLUC), APH treatment moderately affected the recovery of replisome components (~17% decrease). By contrast, APH had a severe impact on the recovery of replisome components from RIF1-depleted cells (~50% decrease for shRIF1 (1) and ~33% decrease for shRIF1 (2)). We conclude that APH treatment reduces the probability to capture proteins associated with EdU-labelled DNA in RIF1-depleted cells. Thus, we propose that in conditions of DNA replication stress, RIF1 maintains the organization of replication factories.

RIF1 is required to maintain the organization of replication factories in presence of replicative stress.

To validate our model using an alternative approach, we performed immunofluorescence microscopy experiments. Replication factories labelled by EdU incorporation form distinct and characteristic patterns during S-phase (Dimitrova & Berezney, 2002). Interestingly, the mid-S pattern is selectively lost in the absence of RIF1, and RIF1 has been proposed to play a major role in replication timing (Yamazaki et al., 2012). Suppression of RIF1, however, does not perturb S phase progression (Yamazaki et al., 2012). The latter study used a thymidine block as a synchronization procedure. This procedure perturbs the pool of nucleotides and induces DNA replication stress. Thus, we hypothesized that the absence of mid-S pattern in RIF1-depleted cells could reflect the disorganization of replication clusters in conditions of DNA replicative stress. We confirmed that the mid-S pattern is selectively lost after a thymidine block in RIF1-depleted cells (Figure 4A, B). However, RIF1 depletion did not alter the mid-S pattern in an asynchronous population of cells (Figure 4B). We conclude that the loss of the mid-S pattern manifests under stressful conditions and is a consequence of the thymidine block. To check if DNA lesions are increased, we analyzed the level of the marker of DNA damage γ-H2A.X. In an asynchronous population of cells, the depletion of RIF1 had no impact on the percentage of γ-H2A.X positive cells (Figure 4A, C). The level of γ-H2A.X positive cells increased after a thymidine block, as the treatment induces DNA replication stress. Suppression of RIF1, however, tripled the percentage of γ-H2A.X positive cells treated with thymidine (6.9% in control versus 24.1% if shRIF1 (1) and 19.1% in shRIF1 (2). The data indicates that RIF1 is required to maintain the organization of replication clusters under stressful conditions and, thereby, limits the accumulation of DNA lesions visualized by γ-H2A.X staining.

Discussion

RIF1 was originally discovered more than 25 years ago in budding yeast as a negative regulator of telomere elongation (Hardy, Sussel et al., 1992). It is now clearly established that RIF1 is a highly conserved protein (Sreesankar, Senthilkumar et al., 2012) involved in telomeres protection, DNA replication, DNA double-strand break repair, transcription and heterochromatin formation (Mattarocci et al., 2016). The links between the seemingly disparate functions of RIF1, however, remain elusive. Here we propose that RIF1 is a key organizing component of replication factories. This model is based on the following findings: (1) RIF1 is associated with replication factories in basal conditions; (2) Suppression of RIF1 strongly reduced the efficacy of proteins isolation on nascent DNA and yet had no noticeable impact on EdU incorporation and replisome stability. (3) DNA replication stress in RIF1-depleted cells modified S phase patterns and increased the level of the DNA damage marker γH2AX. Our model is consistent with the recent finding that RIF1 bridges DNA molecules localized in proximity (Mattarocci, Reinert et al., 2017). Thus, we propose that the main function of RIF1 is to protect the integrity of high-order structures in the nucleus by keeping them in close proximity (Figure 4D). This model explains previous observations.

The maintenance of higher order nuclear structures by RIF1 suggests how suppression of RIF1 perturbs transcription and heterochromatin formation (Dan, Liu et al., 2014, Li, Wang et al., 2017). It is also consistent with the finding that RIF1 associates with Lamin B1 (Foti et al., 2016). A role for RIF1 in safeguarding the integrity replication factories may also explain how RIF1 controls the activation of dormant origins in response to replicative stress (Hiraga, Ly et al., 2017), and prevents the formation of anaphase bridges (Hengeveld, de Boer et al., 2015 , Zaaijer, Shaikh et al., 2016). RIF1 depletion has a strong impact on replication timing (Cornacchia et al., 2012, Foti et al., 2016, Yamazaki et al., 2012), possibly by regulating DDK kinase activation through an interaction with the PP1 phosphatase (Dave et al., 2014, Hiraga et al., 2014, Mattarocci et al., 2014). Alternatively, it has been proposed that the function of RIF1 in the regulation of the replication-timing program could stem from its ability to bind G-quadruplexes and organize chromatin structures (Kanoh et al., 2015). Since the loss of RIF1 induces drastic changes in nuclear organization revealed by chromosome conformation capture methods (Foti et al., 2016), we favor the hypothesis that the impact of RIF1 on replication timing is a consequence of impaired nuclear organization rather than of a defect in the control of DDK kinases. Our model is also compatible with the fact that RIF1 is protecting stalled replication forks from resection by nucleases, perhaps by promoting the organization of a structure that limits the access of nucleases to nascent DNA (Garzón et al., 2019, Ray Chaudhuri et al., 2016).

This study reveals that the organization of replication forks in replication factories contributes to the maintenance of genome integrity under stressful conditions of DNA replication. This protective function is reminiscent of the telomeres capping mechanism. By analogy with its function at yeast telomeres, we would like to propose that RIF1 is uncasing replication factories (Figure 4D). Last, this study illustrates a new application of the iPOND method. It is generally assumed that the iPOND method captures proteins associated with individual replisomes distributed along a linear DNA template. Here we show that the iPOND method is not only efficient to isolate replisome components but also to capture structural components of replication factories stabilized by formaldehyde crosslinking. Future studies using iPOND and other method should provide new insights into the role of the nuclear organization in DNA replication.

Acknowledgements

We thank all the lab members for comments and suggestions on the project and on the manuscript. We are grateful to Antoine Aze for critical reading of the manuscript. We acknowledge the support of the Site de Recherche Intégrée sur le Cancer Montpellier Cancer grant INCa_INSERM_DGOS_12553. This work was supported by a Jeunes Chercheuses Jeunes Chercheurs (JCJC) grant (REPLIBLOCK ANR-17-CE12-0034-01) from the Agence National de la Recherche (ANR) to Cyril Ribeyre and by grants from la Fondation ARC pour la Recherche sur le Cancer (PGA1 RF20180206787) and Merck Sharp and Dohme Avenir (MSD Avenir) to Angelos Constantinou.

Author Contributions

Cyril Ribeyre: conceptualization, data curation, formal analysis, funding acquisition, investigation, visualization, methodology, project administration and writing original draft, review and editing.

Marion Larroque: Larroque: data curation, formal analysis, investigation and methodology.

Christian Larroque: data curation, formal analysis and methodology.

Angelos Constantinou: conceptualization, data curation, supervision, funding acquisition, validation, visualization, methodology, project administration and writing original draft, review and editing.

Conflict of Interest Statement

The authors declare that they have no conflict of interest.

Methods

Cell lines

HeLa S3 (obtained from ATCC) cells were cultured in Dulbecco's modified Eagle's media (DMEM). Culture media was supplemented with 10% fetal bovine serum (Biowest) and penicillin/streptomycin (Sigma-Aldrich). Cells were incubated in a 5% CO_2 at 37°C.

Gene silencing

For RIF1 depletion siRNA oligonucleotides were purchased from Dharmacon (M-027983-01-0005) and transfected using INTERFERin (Polypus transfection). Anti-RIF1 shRNAs (1) and (2) and anti-luciferase shRNA were cloned in pSUPER-EBV and transfected using Lifofectamine 2000 (Thermo-Fisher). Stable cell lines were selected using puromycin.

Western-blot

The proteins were resolved by SDS-PAGE using home-made or precast gels (Bio-Rad) and transferred to a nitrocellulose membrane (GE Healthcare or Bio-Rad). Antibodies against the following proteins were used: Ser345 Phospho-Chk1 (Cell Signaling Technology 2348), Chk1 (Santa Cruz sc-8408), PCNA (Sigma-Aldrich P8825), Ser4/8 Phospho-RPA32 (A300-245A), RPA32 (Calbiochem NA18), TopBP1 (Bethyl A300-111A), BRCA1 (Santacruz sc-642), RIF1 (Bethyl A300-568A-M), MSH2 (Calbiochem NA27), MCM7 (Abcam ab2360).

Co-Immunoprecipitation

Cells were incubated for 30 min in ice in high salt buffer (50 mM Tris Ph 7.5, 300 mM NaCl, 1% Triton, 1 mM DTT). After 10 min centrifugation at 14000g, supernatant were incubated with anti PCNA antibody (Sigma-Aldrich, P8825) or IgG Rabbit (Calbiochem NI01) overnight at 4°C. Magnetic beads coupled with protein G (Life 10004D) were added for 1 hour and washed 5 times with washing buffer (10 mM Hepes, 100 mM KOAc, 0.1 mM MgOAc). Beads were boiled in Laemmli buffer and supernatants were analyzed by Western-blot.

Isolation of proteins on Nascent DNA (iPOND)

iPOND was performed largely as described in (Lossaint et al., 2013, Ribeyre, Zellweger et al., 2016). Briefly, HeLa S3 cells were pulse labeled with 10 μM EdU for 5 min and a 120 min chase was performed with 10 μM thymidine. Cells were fixed with 1% formaldehyde for 5 min followed or not by quenching of formaldehyde by 5 min incubation with 0.125 M glycine. Fixed samples were collected by centrifugation at 2000 rpm for 3 min, washed three times with PBS and stored at -80°C.

Cells were permeabilized with 0.5% triton and click chemistry was used to conjugate biotin-TEG-azide (Eurogentec) to EdU-labelled DNA. Cells were re-suspended in lysis buffer and sonication was performed using a Qsonica sonicator. Biotin conjugated DNA-protein complexes were captured using streptavidin beads (Ademtech). Captured complexes were washed with lysis buffer and high salt. Proteins associated with nascent DNA were eluted under reducing conditions by boiling into SDS sample buffer for 30 min at 95 °C.

DNA fibers labelling

DNA fibers labelling was performed as previously described (Lossaint et al., 2013, Ribeyre et al., 2016). Cells were labeled with 25µM IdU, washed with warm media and exposed to 50 µM CldU. Cells were lysed and DNA fibers were stretched onto glass slides. The DNA fibers were denatured with 2.5 M HCl for 1 hour, washed with PBS and blocked with 2% BSA in PBS-Tween for 60 minutes. IdU replication tracts were revealed with a mouse anti-BrdU/IdU antibody from BD Biosciences (347580) and CldU tracts with a rat anti-BrdU/CldU antibody from Eurobio (ABC117-7513). The following secondary antibodies were used: alexa fluor 488 anti-mouse antibody (Life A21241) and Cy3 anti-rat antibody (Jackson Immunoresearch 712-166-153). Replication tracts lengths were analyzed using ImageJ software. For statistical analysis we used a non-parametrical Mann-Whitney with Prism software.

Immunofluorescence

Cells were plated on glass coverslips and fixed with 4% paraformaldehyde in PBS for 20 min at room temperature. When indicated cells were incubated with EdU (5-ethynyl-2'-deoxyuridine) for the indicated times. PFA-fixed cells were permeabilized with 0.2% Triton X-100 in PBS for 5 min. Primary (anti-phospho histone H2A.X ser 139; Millipore 05-636) and secondary antibody (Anti Mouse Alexa 488) were prepared in PBS with 0.1% Tween and incubations were carried out in a humidified chamber at room temperature (60 min and 30 min, respectively). EdU was coupled with Alexa fluor 555 using Click chemistry. DNA was stained with Hoechst. The cells were mounted on glass slides with Prolong (Life). Cells were analyzed by fluorescence microscopy and quantification of various signals was performed using CellProfiler software (Carpenter, Jones et al., 2006).

Mass Spectrometry Analysis

Mass spectrometry was performed as indicated in (Kumbhar, Vidal-Eychenié et al., 2018). Analysis of raw files was performed using MaxQuant (Cox & Mann, 2008) version 1.5.6.5 using default settings with label-free quantification option enabled. Raw file spectra were

searched against the human UniProt reference database. Protein, peptide, and site false discovery rate (FDR) were adjusted to < 0.01.

References

Aranda S, Rutishauser D, Ernfors P (2014) Identification of a large protein network involved in epigenetic transmission in replicating DNA of embryonic stem cells. *Nucleic Acids Res* 42: 6972-86

Blow JJ, Ge XQ, Jackson DA (2011) How dormant origins promote complete genome replication. *Trends Biochem Sci* 36: 405-14

Buonomo SB, Wu Y, Ferguson D, de Lange T (2009) Mammalian Rif1 contributes to replication stress survival and homology-directed repair. *The Journal of cell biology* 187: 385-98

Carpenter AE, Jones TR, Lamprecht MR, Clarke C, Kang IH, Friman O, Guertin DA, Chang JH, Lindquist RA, Moffat J, Golland P, Sabatini DM (2006) CellProfiler: image analysis software for identifying and quantifying cell phenotypes. *Genome biology* 7: R100

Chapman JR, Barral P, Vannier JB, Borel V, Steger M, Tomas-Loba A, Sartori AA, Adams IR, Batista FD, Boulton SJ (2013) RIF1 is essential for 53BP1-dependent nonhomologous end joining and suppression of DNA double-strand break resection. *Mol Cell* 49: 858-71

Cobb AM, Murray TV, Warren DT, Liu Y, Shanahan CM (2016) Disruption of PCNA-lamins A/C interactions by prelamin A induces DNA replication fork stalling. *Nucleus* 7: 498-511

Cornacchia D, Dileep V, Quivy JP, Foti R, Tili F, Santarella-Mellwig R, Antony C, Almouzni G, Gilbert DM, Buonomo SB (2012) Mouse Rif1 is a key regulator of the replication-timing programme in mammalian cells. *Embo J* 31: 3678-90

Courbet S, Gay S, Arnoult N, Wronka G, Anglana M, Brison O, Debatisse M (2008) Replication fork movement sets chromatin loop size and origin choice in mammalian cells. *Nature* 455: 557-60

Cox J, Mann M (2008) MaxQuant enables high peptide identification rates, individualized p.p.b.-range mass accuracies and proteome-wide protein quantification. *Nature biotechnology* 26: 1367-72

Dan J, Liu Y, Liu N, Chiourea M, Okuka M, Wu T, Ye X, Mou C, Wang L, Wang L, Yin Y, Yuan J, Zuo B, Wang F, Li Z, Pan X, Yin Z, Chen L, Keefe DL, Gagos S et al. (2014) Rif1 maintains telomere length homeostasis of ESCs by mediating heterochromatin silencing. *Developmental cell* 29: 7-19

Dave A, Cooley C, Garg M, Bianchi A (2014) Protein phosphatase 1 recruitment by Rif1 regulates DNA replication origin firing by counteracting DDK activity. *Cell reports* 7: 53-61

Dekker J, Rippe K, Dekker M, Kleckner N (2002) Capturing chromosome conformation. *Science* 295: 1306-11

Dimitrova DS, Berezney R (2002) The spatio-temporal organization of DNA replication sites is identical in primary, immortalized and transformed mammalian cells. *J Cell Sci* 115: 4037-51

Dungrawala H, Rose KL, Bhat KP, Mohni KN, Glick GG, Couch FB, Cortez D (2015) The Replication Checkpoint Prevents Two Types of Fork Collapse without Regulating Replisome Stability. *Mol Cell* 59: 998-1010

Foti R, Gnan S, Cornacchia D, Dileep V, Bulut-Karslioglu A, Diehl S, Buness A, Klein FA, Huber W, Johnstone E, Loos R, Bertone P, Gilbert DM, Manke T, Jenuwein T, Buonomo SC (2016) Nuclear Architecture Organized by Rif1 Underpins the Replication-Timing Program. *Mol Cell* 61: 260-73

Garzón J, Ursich S, Lopes M, Hiraga S-i, Donaldson AD (2019) Human RIF1-Protein Phosphatase 1 Prevents Degradation and Breakage of Nascent DNA on Replication Stalling. *Cell reports* 27: 2558-2566.e4

Guillou E, Ibarra A, Coulon V, Casado-Vela J, Rico D, Casal I, Schwob E, Losada A, Mendez J (2010) Cohesin organizes chromatin loops at DNA replication factories. *Genes Dev* 24: 2812-22

Hardy CF, Sussel L, Shore D (1992) A RAP1-interacting protein involved in transcriptional silencing and telomere length regulation. *Genes Dev* 6: 801-14

Hayano M, Kanoh Y, Matsumoto S, Renard-Guillet C, Shirahige K, Masai H (2012) Rif1 is a global regulator of timing of replication origin firing in fission yeast. *Genes Dev* 26: 137-50

Hengeveld RC, de Boer HR, Schoonen PM, de Vries EG, Lens SM, van Vugt MA (2015) Rif1 Is Required for Resolution of Ultrafine DNA Bridges in Anaphase to Ensure Genomic Stability. *Developmental cell* 34: 466-74

Hiraga S, Alvino GM, Chang F, Lian HY, Sridhar A, Kubota T, Brewer BJ, Weinreich M, Raghuraman MK, Donaldson AD (2014) Rif1 controls DNA replication by directing Protein Phosphatase 1 to reverse Cdc7-mediated phosphorylation of the MCM complex. *Genes Dev* 28: 372-83
Hiraga SI, Ly T, Garzon J, Horejsi Z, Ohkubo YN, Endo A, Obuse C, Boulton SJ, Lamond AI, Donaldson AD (2017) Human RIF1 and protein phosphatase 1 stimulate DNA replication origin licensing but suppress origin activation. *EMBO Rep* 18: 403-419
Hozak P, Hassan AB, Jackson DA, Cook PR (1993) Visualization of replication factories attached to nucleoskeleton. *Cell* 73: 361-73
Jackson DA, Pombo A (1998) Replicon clusters are stable units of chromosome structure: evidence that nuclear organization contributes to the efficient activation and propagation of S phase in human cells. *The Journal of cell biology* 140: 1285-95
Kanoh Y, Matsumoto S, Fukatsu R, Kakusho N, Kono N, Renard-Guillet C, Masuda K, Iida K, Nagasawa K, Shirahige K, Masai H (2015) Rif1 binds to G quadruplexes and suppresses replication over long distances. *Nat Struct Mol Biol* 22: 889-97
Kumbhar R, Vidal-Eychenié S, Kontopoulos D-G, Larroque M, Larroque C, Basbous J, Kossida S, Ribeyre C, Constantinou A (2018) Recruitment of ubiquitin-activating enzyme UBA1 to DNA by poly(ADP-ribose) promotes ATR signalling. *Life Science Alliance* 1
Lambert S, Carr AM (2013) Impediments to replication fork movement: stabilisation, reactivation and genome instability. *Chromosoma* 122: 33-45
Li P, Wang L, Bennett BD, Wang J, Li J, Qin Y, Takaku M, Wade PA, Wong J, Hu G (2017) Rif1 promotes a repressive chromatin state to safeguard against endogenous retrovirus activation. *Nucleic Acids Res* 45: 12723-12738
Lopez-Contreras AJ, Ruppen I, Nieto-Soler M, Murga M, Rodriguez-Acebes S, Remeseiro S, Rodrigo-Perez S, Rojas AM, Mendez J, Munoz J, Fernandez-Capetillo O (2013) A proteomic characterization of factors enriched at nascent DNA molecules. *Cell reports* 3: 1105-16
Lossaint G, Larroque M, Ribeyre C, Bec N, Larroque C, Decaillet C, Gari K, Constantinou A (2013) FANCD2 binds MCM proteins and controls replisome function upon activation of s phase checkpoint signaling. *Mol Cell* 51: 678-90
Mattarocci S, Hafner L, Lezaja A, Shyian M, Shore D (2016) Rif1: A Conserved Regulator of DNA Replication and Repair Hijacked by Telomeres in Yeasts. *Frontiers in genetics* 7: 45
Mattarocci S, Reinert JK, Bunker RD, Fontana GA, Shi T, Klein D, Cavadini S, Faty M, Shyian M, Hafner L, Shore D, Thoma NH, Rass U (2017) Rif1 maintains telomeres and mediates DNA repair by encasing DNA ends. *Nat Struct Mol Biol* 24: 588-595
Mattarocci S, Shyian M, Lemmens L, Damay P, Altintas DM, Shi T, Bartholomew CR, Thoma NH, Hardy CF, Shore D (2014) Rif1 controls DNA replication timing in yeast through the PP1 phosphatase Glc7. *Cell reports* 7: 62-9
Mechali M (2010) Eukaryotic DNA replication origins: many choices for appropriate answers. *Nat Rev Mol Cell Biol* 11: 728-38
Moriyama K, Yoshizawa-Sugata N, Masai H (2018) Oligomer formation and G-quadruplex binding by purified murine Rif1 protein, a key organizer of higher-order chromatin architecture. *J Biol Chem* 293: 3607-3624
Munden A, Rong Z, Sun A, Gangula R, Mallal S, Nordman JT (2018) Rif1 inhibits replication fork progression and controls DNA copy number in Drosophila. *Elife* 7
Ray Chaudhuri A, Callen E, Ding X, Gogola E, Duarte AA, Lee JE, Wong N, Lafarga V, Calvo JA, Panzarino NJ, John S, Day A, Crespo AV, Shen B, Starnes LM, de Ruiter JR, Daniel JA, Konstantinopoulos PA, Cortez D, Cantor SB et al. (2016) Replication fork stability confers chemoresistance in BRCA-deficient cells. *Nature* 535: 382-7
Ribeyre C, Zellweger R, Chauvin M, Bec N, Larroque C, Lopes M, Constantinou A (2016) Nascent DNA Proteomics Reveals a Chromatin Remodeler Required for Topoisomerase I Loading at Replication Forks. *Cell reports* 15: 300-9

Ryba T, Hiratani I, Lu J, Itoh M, Kulik M, Zhang J, Schulz TC, Robins AJ, Dalton S, Gilbert DM (2010) Evolutionarily conserved replication timing profiles predict long-range chromatin interactions and distinguish closely related cell types. *Genome research* 20: 761-70
Singh M, Hunt CR, Pandita RK, Kumar R, Yang CR, Horikoshi N, Bachoo R, Serag S, Story MD, Shay JW, Powell SN, Gupta A, Jeffery J, Pandita S, Chen BP, Deckbar D, Lobrich M, Yang Q, Khanna KK, Worman HJ et al. (2013) Lamin A/C depletion enhances DNA damage-induced stalled replication fork arrest. *Mol Cell Biol* 33: 1210-22
Sirbu BM, Couch FB, Feigerle JT, Bhaskara S, Hiebert SW, Cortez D (2011) Analysis of protein dynamics at active, stalled, and collapsed replication forks. *Genes Dev* 25: 1320-7
Sirbu BM, McDonald WH, Dungrawala H, Badu-Nkansah A, Kavanaugh GM, Chen Y, Tabb DL, Cortez D (2013) Identification of proteins at active, stalled, and collapsed replication forks using isolation of proteins on nascent DNA (iPOND) coupled with mass spectrometry. *J Biol Chem* 288: 31458-67
Sreesankar E, Senthilkumar R, Bharathi V, Mishra RK, Mishra K (2012) Functional diversification of yeast telomere associated protein, Rif1, in higher eukaryotes. *BMC genomics* 13: 255
Tittel-Elmer M, Lengronne A, Davidson MB, Bacal J, Francois P, Hohl M, Petrini JH, Pasero P, Cobb JA (2012) Cohesin association to replication sites depends on rad50 and promotes fork restart. *Mol Cell* 48: 98-108
Wheaton K, Campuzano D, Ma W, Sheinis M, Ho B, Brown GW, Benchimol S (2017) Progerin-Induced Replication Stress Facilitates Premature Senescence in Hutchinson-Gilford Progeria Syndrome. *Mol Cell Biol* 37
Xu D, Muniandy P, Leo E, Yin J, Thangavel S, Shen X, Ii M, Agama K, Guo R, Fox D, 3rd, Meetei AR, Wilson L, Nguyen H, Weng NP, Brill SJ, Li L, Vindigni A, Pommier Y, Seidman M, Wang W (2010) Rif1 provides a new DNA-binding interface for the Bloom syndrome complex to maintain normal replication. *Embo J* 29: 3140-55
Yamazaki S, Hayano M, Masai H (2013) Replication timing regulation of eukaryotic replicons: Rif1 as a global regulator of replication timing. *Trends Genet* 29: 449-60
Yamazaki S, Ishii A, Kanoh Y, Oda M, Nishito Y, Masai H (2012) Rif1 regulates the replication timing domains on the human genome. *EMBO J* 31: 3667-77
Zaaijer S, Shaikh N, Nageshan RK, Cooper JP (2016) Rif1 Regulates the Fate of DNA Entanglements during Mitosis. *Cell reports* 16: 148-60
Zeman MK, Cimprich KA (2014) Causes and consequences of replication stress. *Nat Cell Biol* 16: 2-9

Figures Legends

Figure 1: RIF1 is associated with ongoing replisomes under basic conditions. A. iPOND coupled with mass spectrometry (label-free quantification using MaxQuant). HeLa S3 cells were pulse-labelled with EdU for 5 min and chased with thymidine for 120 min. The bar plot is showing the LogRatio (pulse/chase) of average peptides intensities corresponding to indicated proteins. Pulse experiment has been repeated 3 times and chase experiment 2 times. **B.** Indicated proteins were isolated by iPOND and detected by Western blotting. HeLa S3 cells were pulse-labelled with EdU for 15 min and chased with thymidine for 120 min. In no click samples (no Clk), biotin-TEG azide was replaced by DMSO. **C.** Western-blot analysis of indicated proteins after immunoprecipitation with an antibody directed against PCNA or against mouse IgG. **D.** Western-blot analysis of indicated proteins upon transfection with siRNA directed against RIF1 or a control target.

Figure 2: Aphidicolin increases DNA lesions in absence of RIF1. A. DNA fibers labelling. HeLa S3 cells were labelled for 30 min with IdU and then for 30 min with CldU in the absence or presence of 0.05 μM aphidicolin (APH) in the cell culture medium. Graphic representation of the ratios of CldU versus IdU tract length. The horizontal bar represents the median with the value indicated in red. 50 replication tracts were measured for each experimental condition. The second graphic representation is showing the medians of three independent experiments. **B.** Analysis of DNA resection using DNA fibers labelling. HeLa S3 cells were labelled for 30 min with IdU and then for 30 min with CldU. 1 μM aphidicolin (APH) was added in the cell culture medium for 6 hours. Graphic representation of the ratios of CldU versus IdU tract length. The horizontal bar represents the median with the value indicated in red. 50 replication tracts were measured for each experimental condition. **C.** Immunofluorescence analysis of γH2A.X and RIF1 in HeLa S3 cells with siRNA against control or RIF1 in presence or absence of aphidicolin (APH) for 24 hours. **D.** Graphic representation of the quantification of γH2A.X intensity within nucleus stained with Hoechst using CellProfiler based on three independent experiments for each conditions.

Figure 3: RIF1 loss reduces the association of replisome components with EdU in response to replicative stress. A. iPOND efficiency may be related to proteins density around EdU-labelled DNA. **B.** Western-blot analysis of indicated proteins in HeLa S3 stable cell lines expressing a shRNA against luciferase (LUC) or two different shRNA against RIF1. **C.** iPOND experiment. HeLa S3 cells (with shLUC or two different shRIF1) were labelled with EdU for 15 min or for 30 min with 0.1 μM aphidicolin (APH). Indicated proteins were analyzed by Western-blot. In no click samples (no Clk), biotin-TEG azide was replaced by DMSO. **D.** iPOND experiment. HeLa S3 cells (with shLUC or two different shRIF1) were treated 30 min with 0.1 μM aphidicolin (APH) then washed and labelled with EdU for 30

min. Indicated proteins were analyzed by Western-blot. In no click samples (no Clk), biotin-TEG azide was replaced by DMSO. **E, F.** iPOND-MS analysis. HeLa S3 cells (with shLUC or two different shRIF1) were labelled with EdU for 15 min or for 30 min EdU with 0.1 μM aphidicolin (APH). Quantification of peptides intensity corresponding to the indicated proteins is represented. **G.** Summed intensities of peptides corresponding to replisomes components.

Figure 4: RIF1 is required to maintain the organization of replication factories in response to replicative stress. A. Immunofluorescence analysis of γH2A.X and EdU in asynchronous cells and in cells synchronized with thymidine block in HeLa S3 cells with shRNA against luciferase or RIF1. **B.** Graphic representation of the frequency of replication patterns (Late-S, Mid-S and Early-S) based on at least three independent experiments for each conditions. **C.** Quantification of γH2A.X intensity within nucleus stained with Hoechst using CellProfiler based on at least three independent experiments for each conditions. **D.** Model to explain the new function of RIF1 in protection of replication factories.

SupData1: DNA fibers labelling. HeLa S3 cells were labelled for 30 min with IdU and then for 30 min with CldU. Graphic representation of the ratios of CldU tract length. The horizontal bar represents the median with the value indicated in red. At least 50 replication tracts were measured for each experimental condition. The second graphic representation is showing the medians of three independent experiments.

SupData2: A. DNA fibers labelling. HeLa S3 cells were labelled for 30 min with IdU and then for 30 min with CldU in the absence or presence of 0.05 μM aphidicolin (APH) in the cell culture medium. Graphic representation of the ratios of CldU versus IdU tract length. The horizontal bar represents the median with the value indicated in red. At least 50 replication tracts were measured for each experimental condition. **B.** Analysis of EdU incorporation using microscopy in HeLa S3 cells with shRNA against luciferase or RIF1. EdU was incorporated in cells during 15 min with or without 0.1 μM aphidicolin (APH). Quantification of EdU intensity within nucleus stained with Hoechst was performed using CellProfiler and is represented on the histogram. Error-bars corresponds to the average values of three independent experiments. **C.** Western-blot analysis of indicated proteins after immunoprecipitation with an antibody directed against PCNA or against mouse IgG. When indicated HeLa S3 cells (shLUc or shRIF1) were treated for 30 min with 0.1 μM aphidicolin (APH).

Figure 1

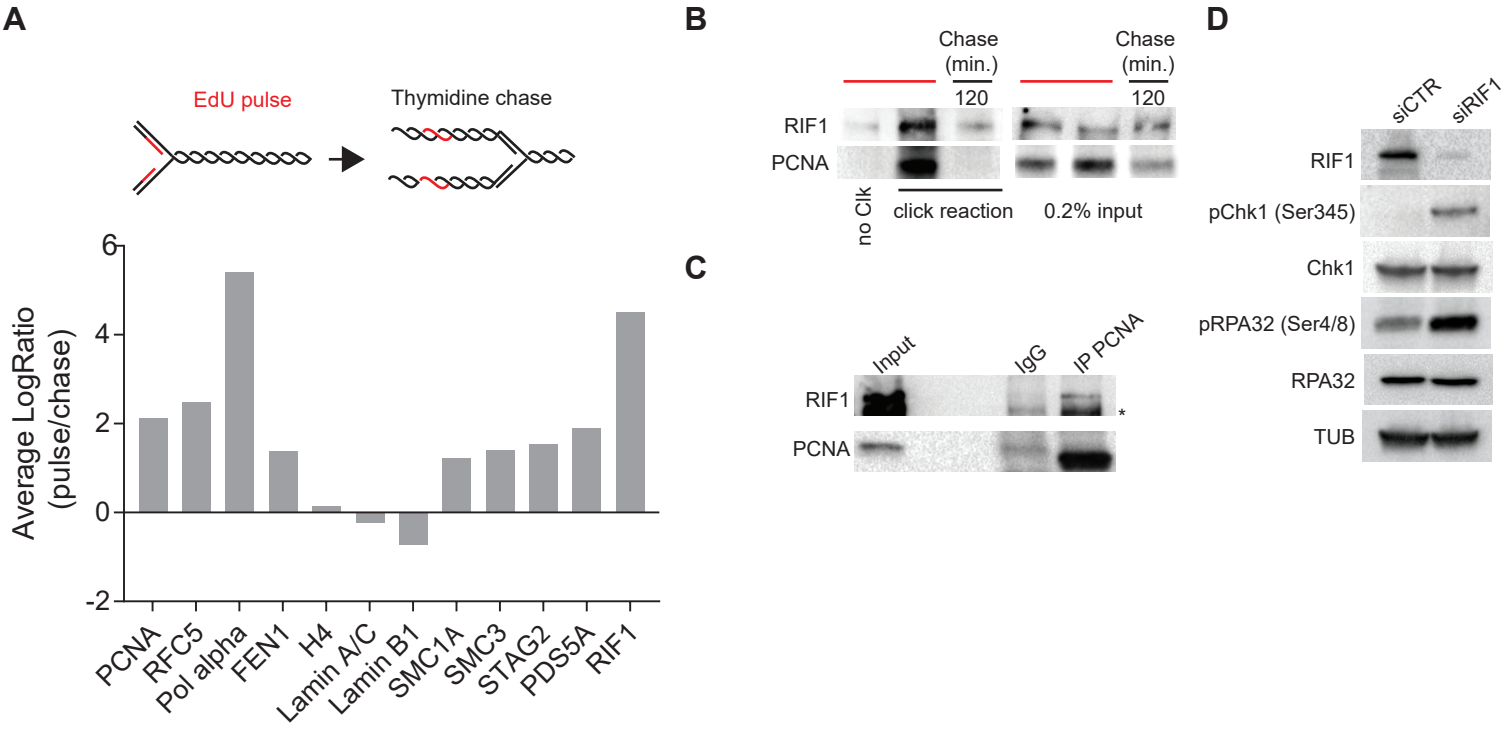
A
EdU pulse
Thymidine chase
Average LogRatio (pulse/chase)
6
4
2
0
-2
PCNA
RFC5
Pol alpha
FEN1
H4
Lamin A/C
Lamin B1
SMC1A
SMC3
STAG2
PDS5A
RIF1
B
Chase (min.)
120
Chase (min.)
120
RIF1
PCNA
no Clk
click reaction
0.2% input
C
Input
IgG
IP PCNA
RIF1
PCNA
*
D
siCTR
siRIF1
RIF1
pChk1 (Ser345)
Chk1
pRPA32 (Ser4/8)
RPA32
TUB

Figure 2

A

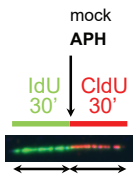

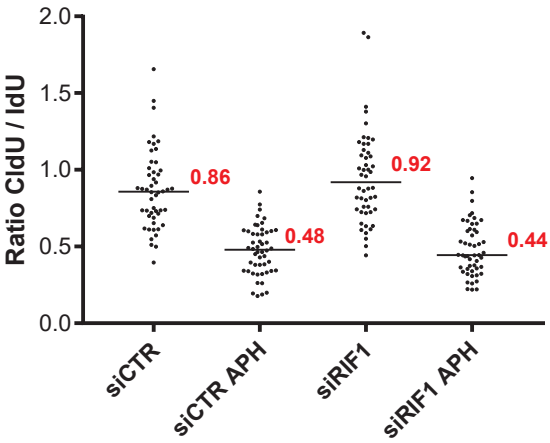

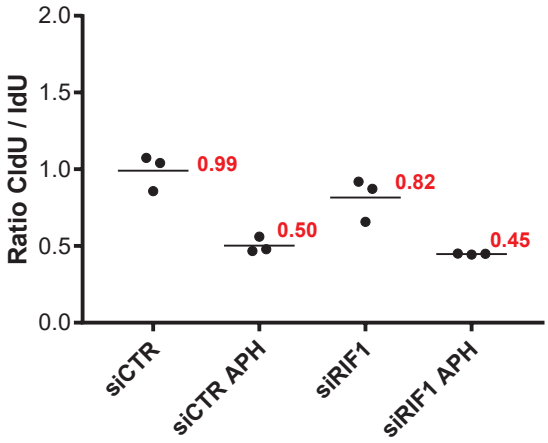

B

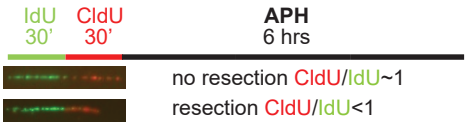

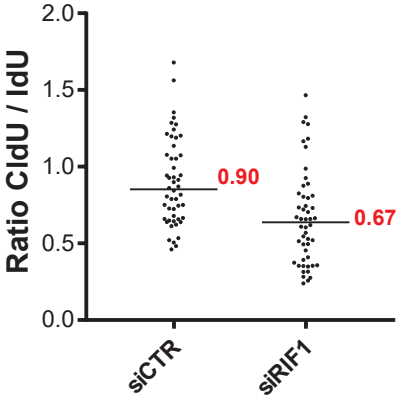

C

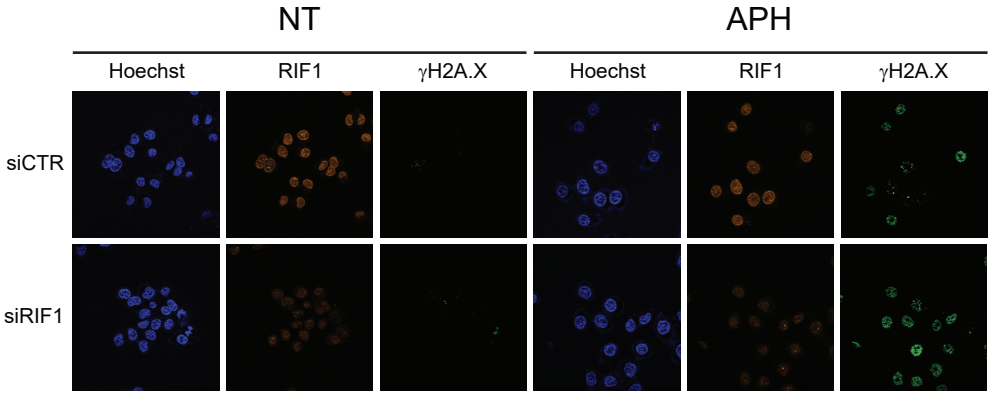

D

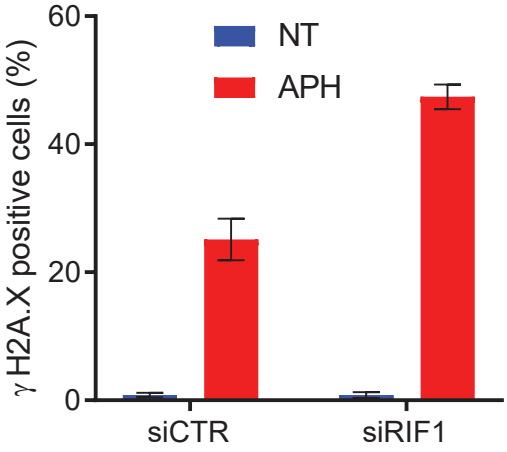

Figure 3

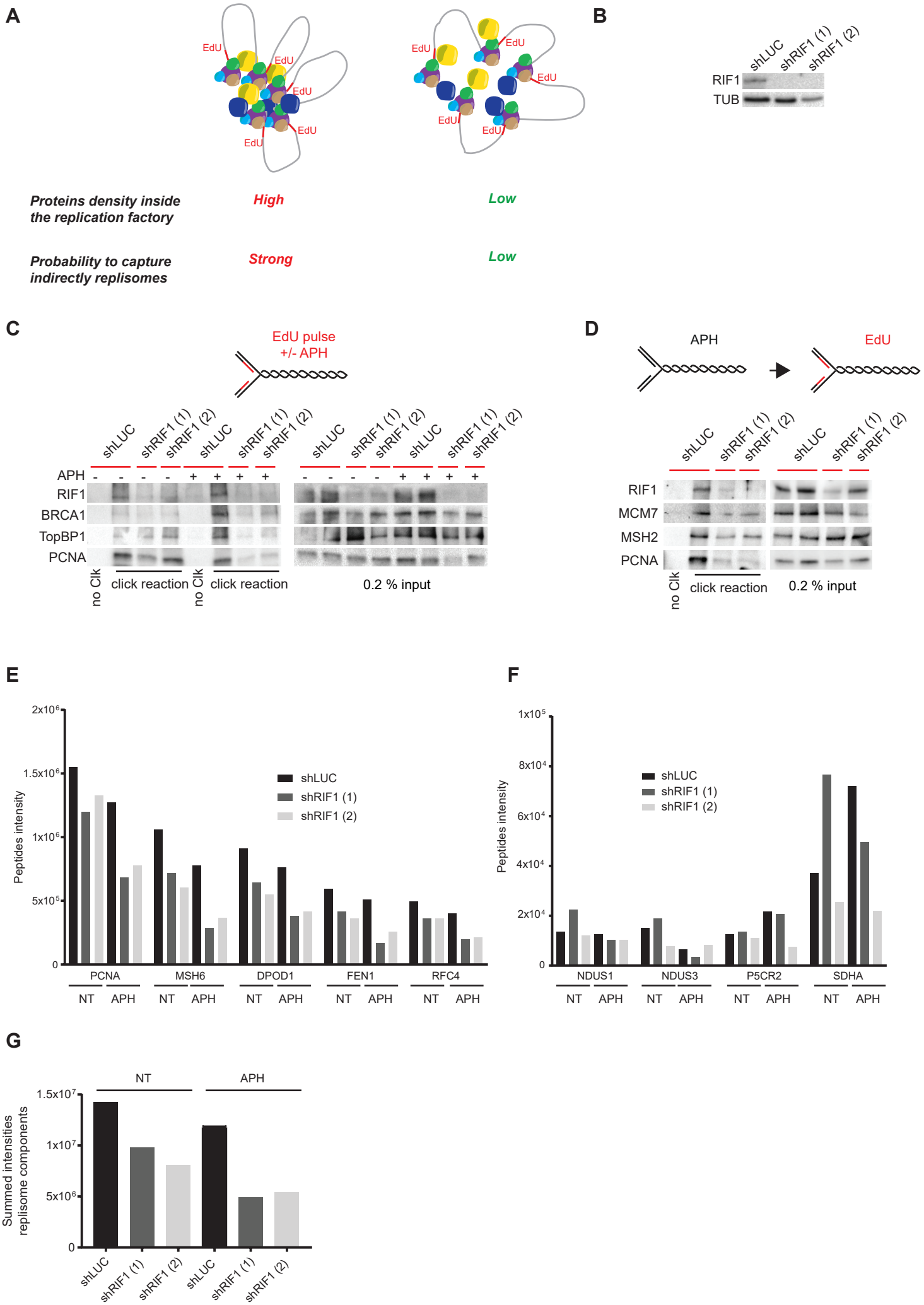
A
EdU
Proteins density inside the replication factory
High
Low
Probability to capture indirectly replisomes
Strong
Low
B
shLUC
shRIF1 (1)
shRIF1 (2)
RIF1
TUB
C
EdU pulse +/- APH
APH
RIF1
BRCA1
TopBP1
PCNA
no Clk
click reaction
0.2 % input
D
APH
EdU
RIF1
MCM7
MSH2
PCNA
no Clk
click reaction
0.2 % input
E
Peptides intensity
shLUC
shRIF1 (1)
shRIF1 (2)
PCNA
MSH6
DPOD1
FEN1
RFC4
NT
APH
F
Peptides intensity
NDUS1
NDUS3
P5CR2
SDHA
G
Summed intensities replisome components
NT
APH

Figure 4

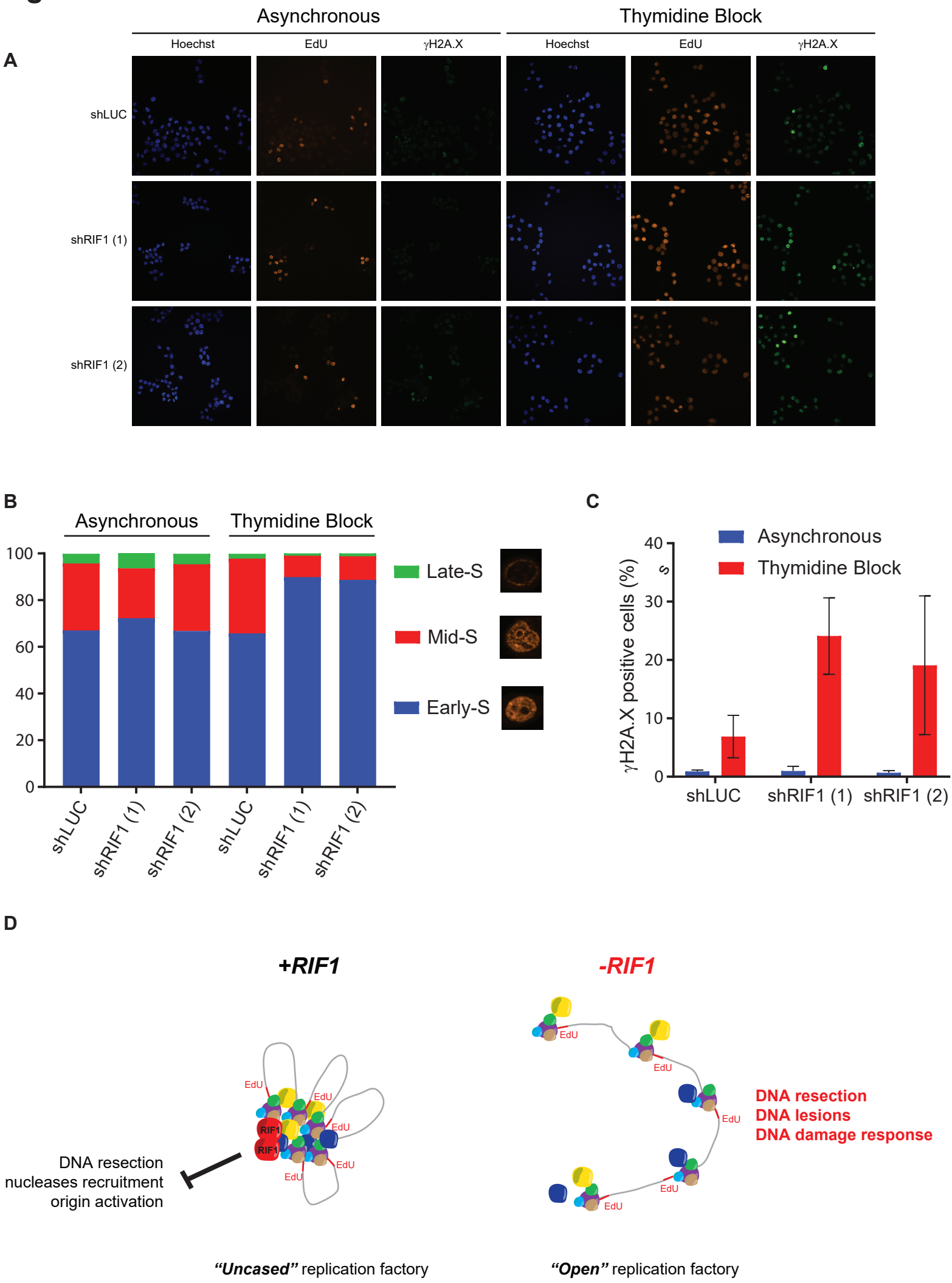
A
Asynchronous
Thymidine Block
Hoechst
EdU
γH2A.X
shLUC
shRIF1 (1)
shRIF1 (2)
B
Asynchronous
Thymidine Block
100
80
60
40
20
0
Late-S
Mid-S
Early-S
shLUC
shRIF1 (1)
shRIF1 (2)
C
Asynchronous
Thymidine Block
γH2A.X positive cells (%)
40
30
20
10
0
shLUC
shRIF1 (1)
shRIF1 (2)
D
+RIF1
-RIF1
EdU
RIF1
DNA resection
nucleases recruitment
origin activation
DNA resection
DNA lesions
DNA damage response
"Uncased" replication factory
"Open" replication factory

SupFig1

A

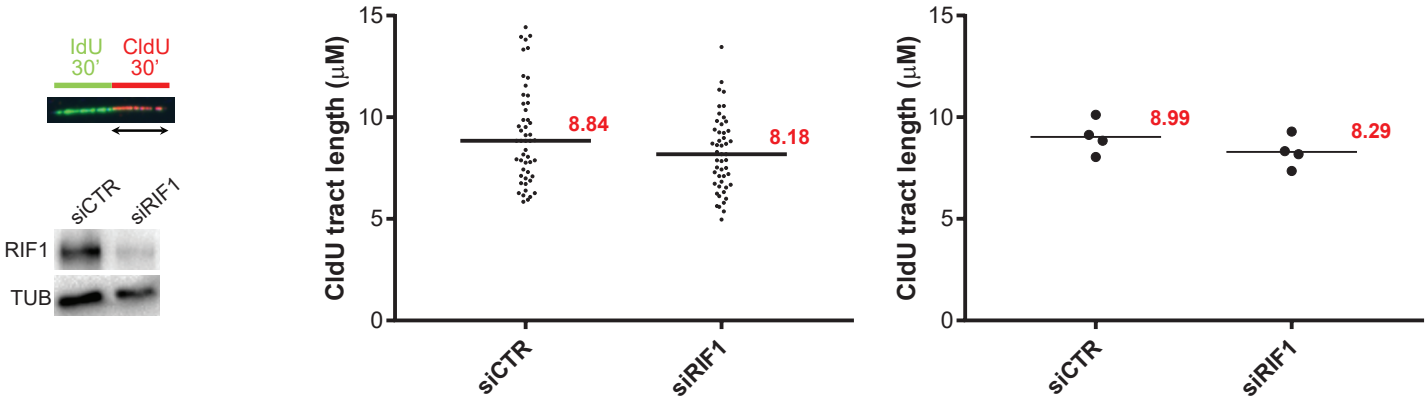
IdU 30'
CldU 30'
siCTR
siRIF1
RIF1
TUB
CldU tract length (μM)
15
10
5
0
8.84
8.18
siCTR
siRIF1
CldU tract length (μM)
15
10
5
0
8.99
8.29
siCTR
siRIF1

SupFig2

A

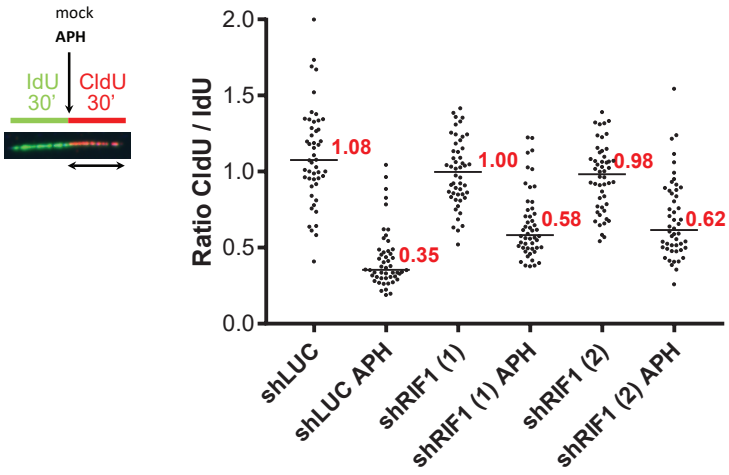
mock
APH
IdU 30'
CldU 30'
Ratio CldU / IdU
2.0
1.5
1.0
0.5
0.0
1.08
0.35
1.00
0.58
0.98
0.62
shLUC
shLUC APH
shRIF1 (1)
shRIF1 (1) APH
shRIF1 (2)
shRIF1 (2) APH

B

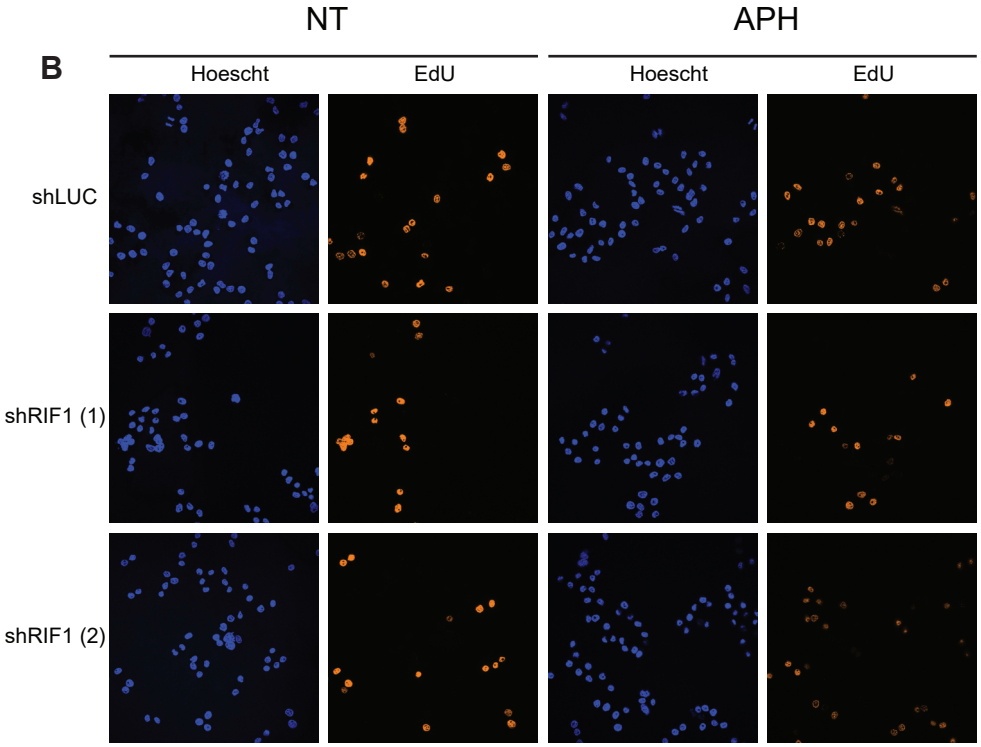
NT
APH
Hoescht
EdU
Hoescht
EdU
shLUC
shRIF1 (1)
shRIF1 (2)

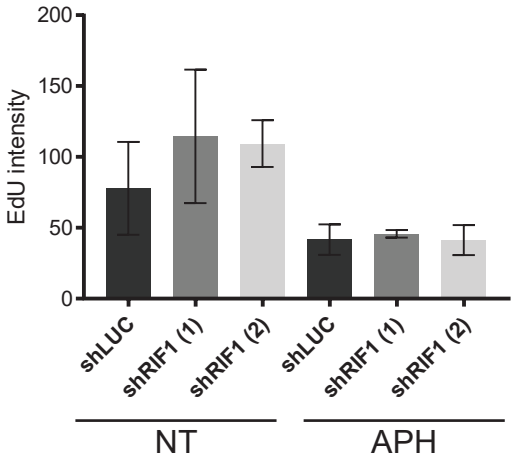
EdU intensity
200
150
100
50
0
shLUC
shRIF1 (1)
shRIF1 (2)
shLUC
shRIF1 (1)
shRIF1 (2)
NT
APH

C

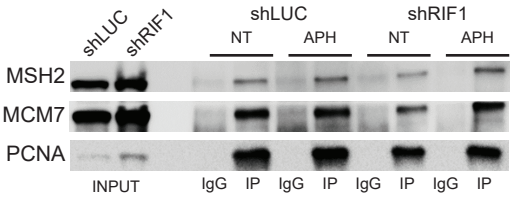
shLUC
shRIF1
shLUC
NT
APH
shRIF1
NT
APH
MSH2
MCM7
PCNA
INPUT
IgG
IP
IgG
IP
IgG
IP
IgG
IP